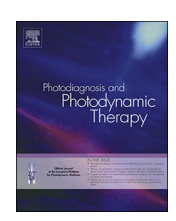
ELSEVIER

Contents lists available at ScienceDirect

Photodiagnosis and Photodynamic Therapy

journal homepage: www.elsevier.com/locate/pdpdt



Investigation of the emission spectra and cytotoxicity of TiO₂ and Ti-MSN/PpIX nanoparticles to induce photodynamic effects using X-ray



Atefeh Vejdani Noghreiyan^{a,b}, Mohammad Reza Sazegar^{c,*}, <mark>Seyed Ali Mousavi Shaegh^{d,e,g},</mark> Ameneh Sazgarnia^f

- ^a Student Research Committee, Mashhad University of Medical Sciences, Mashhad, Iran
- Department of Medical Physics, Faculty of Medicine, University of Medical Sciences, Mashhad, Iran
- ^c Department of Chemistry, Islamic Azad University, North Tehran Branch, Hakimiyeh, Tehran, Iran
- ^d Orthopedic Research Center, Mashhad University of Medical Sciences, Mashhad, Iran
- ^e Clinical Research Unit, Mashhad University of Medical Sciences, Mashhad, Iran
- f Medical Physics Research Center, Mashhad University of Medical Sciences, Mashhad, Iran
- ^g Laboratory of Microfluidics and Medical Microsystems, BuAli Research Institute, Mashhad University of Medical Sciences

ARTICLE INFO

Keywords: Ti-MSN/PpIX nanoparticles TiO₂ Emission spectrum X-ray Photodynamic therapy X-PDT X-rays

ABSTRACT

Background: Photodynamic therapy (PDT) has been recognized as an effective method for cancer treatment; however, it suffers from limited tissue penetration depth. X-rays are ideal excitation sources for activating self-lighting nanoparticles that can penetrate through deep tumor tissues and convert the X-rays to visible light. In this study, Ti-MSN/PpIX nanoparticles for X-ray induced photodynamic therapy was synthesized. Preparation, characterization, and emission spectrum of Ti-MSN/PpIX nanoparticles as well as PDT activity and toxicity of the nanoparticles on HT-29 cell line were investigated.

Methods: Firstly, mesoporous silica nanoparticles (MSN) were synthesized through sol-gel method. Then, TiO_2 and PpIX were loaded in MSN. Next, the emission spectra of TiO_2 , Ti-MSN, and Ti-MSN/PpIX nanoparticles, while activated by X-ray (6 MV $_p$), were recorded. In addition, viability of cells after treatment by Ti-MSN/PpIX nanoparticles and X-ray irradiation was studied.

Results: SEM, TEM and FESEM images of the spherical composite nanoparticles showed that their dimensions were changed by incorporating Ti and organic compound of PpIX. Two-dimensional hexagonal structure with d_{100} -spacing was about 3.5 nm with particle sizes of 70-110 nm. The optical characteristics of TiO_2 nanoparticles showed strong emission lines, which effectively overlapped with the absorption wavelengths of protoporphyrin IX (PpIX). Cellular experiments showed Ti-MSN/PpIX nanoparticles have proper biocompatibility, however, after X-ray irradiation, significant decrease of cell viability in the presence of the nanoparticles was observed.

Conclusion: The presented X-PDT method could enhance RT efficacy and is enable that allows for reducing X-ray dose exposure to healthy tissues to overcome radio-resistant tumors.

1. Introduction

Radiotherapy is considered as one of the efficacious methods for the treatment of malignant tumors, but it may induce side effects for surrounding tissues. In contrast to radiotherapy, PDT is recognized as a safe therapeutic method with potentially limited damage to adjacent healthy tissues [1,2].

In PDT, three components are necessary; photosensitizer (PS), oxygen and light with appropriate wavelength. A photosensitizer (PS) in presence of oxygen, generates reactive oxygen species under light

irradiation to damage cancer cells [3,4]. However, the use of PDT is restricted to accessible tissues due to limited penetration depth of light. To enhance the penetration depth and decrease the radiotherapy dose, several studies have to provide efficient treatments through combining radiotherapy and photodynamic therapy (RT-PDT, or X-PDT) [5–7]. In this way, several kinds of PSs including metallic phthalocyanines, chlorines, phenothiazinium components and porphyrins have been developed for PDT [8].

Majority of such photosensitizers have hydrophobic properties that may induce aggregate formation after blood injection, and decrease the

E-mail addresses: Vejdania931@mums.ac.ir (A. Vejdani Noghreiyan), m_r_sazegar@yahoo.com (M.R. Sazegar).

^{*} Corresponding author.

efficiency of PDT [9]. To try to resolve this issue, one might synthesize water soluble PS compounds in order to enhance drug uptake by cancer cells [10].

Nano carriers are able to protect PS components from agglomeration at physiological conditions of target cells environment. Mesoporous silica nanoparticles (MSN) and their modified nanostructures could be employed as proper carriers for PS due to their unique features such as large surface area, high pore volume, hydrothermal stability and biocompatibility [11,12].

The growth of medicinal nanotechnology has enabled to overcome the limitations of PDT through combining two modalities in a therapeutic method.

To this end, in the present study, MSNs were used as PS and self-lighting carrier nanoparticles. MSNs are optically transparent which this property causes they don't absorb the light emitted from self-lighting nanoparticles (TiO₂). Since there is no PS that can directly absorb X-ray energy, self-lighting nanoparticles were used to convert X-rays to visible light to induce X-PDT [6,13,14]. To this end, a novel nanocomposite based on TiO₂-grafted mesoporous silica nanostructure functionalized with PpIX compound, denoted as Ti-MSN/PpIX, was designed and synthesized. X-ray luminescence of TiO₂ nanoparticles was used in order to excite PpIX molecules as a photosensitizer. Under ionizing radiation exposure, TiO₂ emits persistent luminescence that activates PpIX. The outcome is the generation of cytotoxic singlet oxygen (1 O₂), which causes cell death.

The combination of radiotherapy and PDT could provide a low-cost and efficacious treatment method with the benefits of radiotherapy at lower doses [6]. These two modalities could be sufficient to attack both cell membrane, the target point of PDT, and DNA -RT endpoint- causing lethal damage [5]. Besides, the limitation of treatment depth of PDT could be enhanced and allowing for the treatment of both shallow and deep tumors.

In this study, the characterization of the nanocomposite was carried out using Fourier-transform infrared spectroscopy (FTIR), X-ray diffraction (XRD), scanning electron microscopy (SEM) and Brunauer-Emmett-Teller (BET) analysis. The emitted spectrum of TiO₂, while excited by X-rays, was recorded and compared to absorption spectrum of PpIX. And finally, the effect of the synthesized nanostructures on the cell line was investigated.

2. Materials and methods

Tetraethylorthosilicate (TEOS, 98 %, Merck) was used as silica source for the synthesis of the pure MSN. Cetyltrimethyl ammonium bromide (CTAB, 99 %, Merck) was a cationic surfactant used as a template in the synthesis of MSN. Titanium oxide (Anatase type) was used as a self-lighting nanomaterial. Protoporphyrin IX (PpIX, 95 %, Sigma-Aldrich) was purchased as a source of photosensitizer for photodynamic therapy. Ethylene glycol (EG) and 1,2-propanediol (PD) were employed as the co-solvent materials. Ethanol, ammonia and other reagents were obtained from Merck. Required deionized water was produced by a Milli-Q system. All the chemicals were of analytical grade and applied as obtained, without further purification.

2.1. MSN synthesis

MSN were prepared using cetyltrimethyl ammonium bromide (CTAB) as surfactant, tetraethyl orthosilicate (TEOS) as a source of siliceous and ethylene glycol (EG) along with 1,2-propanediol (PD) as cosolvents for sol-gel method. CTAB (3.2 mmol, 1.17 g) was dissolved in an aqueous solution including double distilled water (DW, 11 mol, 200 mL), EG (1.25 mol, 70 mL) and PD (0.4 mol, 30 mL) in an aqueous ammonia solution (8.2 mL, 25 %). After stirring for 60 min at 323 K, TEOS (10 mmol, 2.2 mL) was added to the mixture. The mixture was stirred for another 4 h at 50 °C and allowed to age for 24 h. The sample was collected by centrifugation for 45 min at 20,000 rpm and washed

with deionized water (DI) and absolute ethanol for 3 times. The remained CTAB was removed by heating MSN (1 g) in an NH₄NO $_3$ (0.5 g) and ethanol (100 mL) solution at 333 K. The results were collected by centrifugation and dried at 373 K for 10 h followed by calcined in air at 600 °C for 5 h.

2.2. Synthesis of Ti-MSN

The active site of titanium was formed in the framework by using titanium dioxide (TiO₂, Anatase form) as a source of titanium. TiO₂ (4.5 mmol) was dispersed in 100 mL of DW. Then MSN (2 g) was added to the mixture and stirred at 25 °C for 10 h. The obtained mixture was centrifuged with 20,000 rpm for 30 min and dried for 8 h at 363 K followed by calcined for 5 h at 600 °C.

2.3. Synthesis of Ti-MSN/PpIX nanocomposite

Initially, PpIX (0.0046 mmol, 0.0026 g) was dissolved in DMSO (50 mL). Then, Ti-MSN sample (2 g) was added to the solution and stirred for 6 h at 70 $^{\circ}$ C. The product then centrifuged for 25 min and then dried for 8 h at 70 $^{\circ}$ C.

2.4. Characterization of the synthesized nanocomposite

The crystallinity of samples (XRD analysis) was measured using a Bruker Advance D8 X-ray powder diffractometer with Cu K α (λ = 1.5418 Å) radiation as the diffracted monochromatic beam at 40 kV and 40 mA. Nitrogen physisorption analysis was used on a Quantachrome Autosorb-1 at 77 K. Before the measurement, the sample was evacuated at 300 °C for 3 h.

Fourier transform infrared (FTIR) measurements were carried out using an Agilent Carry 640 FTIR spectrometer. The catalyst was prepared as a self-supported wafer and activated under vacuum for 3 h at 400 $^{\circ}$ C [15].

UV–Vis spectra were obtained on a Thermo Spectronic spectrophotometer model Genesys 10 UV, from 300 to 700 nm using a 1 cm quartz cuvette.

The morphology of all samples was determined using a scanning electron microscope (SEM KYKY-EM-3200) operating at an accelerating voltage of 26 kV.

To investigate luminescence emission of TiO_2 nanoparticles and nanocomposite, excited by X-ray, a spectrometer (Avaspec-2048 Dual Thermo-Electric Cooled Fiber Optic; Netherlands) was used.

A linear accelerator (Varian, Linac 600, serial number: 475, California, USA) with the energy of 6 MVp and the irradiation dose of 100 cGy was used to irradiate the samples. Photo-emission recording of each sample was repeated for three samples.

Samples were dispersed in distilled water and then placed in cuvette when its distance from the spectrometer probe for irradiation by X-ray was 2-3 cm. The set-up of photo-emission recording is shown in Fig. 1.

2.5. In vitro experiments

2.5.1. Cytotoxicity assay

To determine the cytotoxicity of the Ti-MSN/PpIX nanoparticles, in vitro experiments in the presence and absence of the nanocomposites were performed. HT-29 cell line, a human colorectal adenocarcinoma cell line, was used.

The cells were grown in RPMI-1640 that supplemented with 10 % (v/v) fetal bovine serum (FBS), 1 % penicillin/streptomycin. The cells were cultured and proliferated in 75 cm² culture flasks as monolayer in a 37 °C incubator with 5 % CO2. After trypsinization of the cells and determining the cell survival using trypan-blue and a light microscope dye, 12×10^3 live cells were seeded in each well of a 96-well plate. 24 h later, culture medium was refreshed and different concentrations of Ti-MSN/PpIX (0.03, 0.07, 0.35, 1.06, 3.19, and 5.31 mg/mL) was added



Fig. 1. The set-up of photo-emission recording during X-ray irradiation by a Linac

to the cells and incubation was continued for 3 h. Next, the cells were washed with phosphate-buffered saline (PBS) and fresh culture medium was added to the wells. MTT (3-[4,5-dimethylthiazol-2-yl]-2, 5-diphenyl tetrazolium bromide) assay was carried out to determine the cell survival after 24 h.

2.5.2. X-Ray and PDT (X-PDT) experiments

The impact of X-PDT on cells was investigated by MTT assay. Cells $(1 \times 10^{4} \text{ cells/well})$ were seeded in seven 96-well plates and incubated overnight. Then, the cells in separate groups were incubated with Ti-MSN/PpIX nanoparticles at the concentration in 90 % cell survival (3.68 mg/mL) for 3 h. A control group with no additive, and a group incubated with Ti-MSN were examined, as well. The concentration of Ti-MSN nanoparticles was considered equal to the group receiving Ti-MSN/PpIX. After washing the cells with PBS, six of the plates were exposed to different doses of 100 kVp and 6 MVp X-ray radiation, separately (1, 2 and 4 Gy). After 48 h incubation, cell viability was evaluated by MTT assay. 5 mg/mL of MTT solution were added and incubated for 4 h at 37 $^{\circ}\text{C},$ afterward the supernatant was taken and 200 μL DMSO was added to cells to lyse them. The cell viability was then calculated as a percentage of the optical density (OD) of each sample relative to the untreated control, which was set to 100 %, at the wavelength of 570 nm against 630 nm.

3. Results

3.1. Physical properties of the catalysts

Fig. 2 shows the XRD pattern of the MSN, Ti-MSN and Ti-MSN/PpIX samples. These samples have showed three peaks of 100, 110 and 200 at 2.25°, 4.30° and 4.60°, respectively. The sharp peaks at 2.30° reveals the ordered crystalline structure that confirmed the 2D hexagonal (p6mm) structure with d_{100} spacing of around 3–5 nm [16]. The XRD pattern exhibited that the peak intensities were decreased after loading of Ti and PpIX materials that indicated to the presence of higher ordered structure in MSN and less crystallinity in the composite. This is evidence to the presence of a non-porous structure of Ti-MSN/PpIX due to the loading of macromolecule structure of PpIX compound onto the Ti-MSN surface.

TEM image of Ti-MSN/PpIX is shown in Fig. 3. The Ti-MSN/PpIX sample consists of spherical monolithic grains. The composite framework based on silica mesoporous is wormhole-like throughout the grain.

Fig. 4 shows SEM images of the MSN, Ti-MSN and Ti-MSN/PpIX and Fig. 5 shows field emission scanning electron microscope (FESEM) images of the Ti-MSN/PpIX composite that exhibits spherical particles

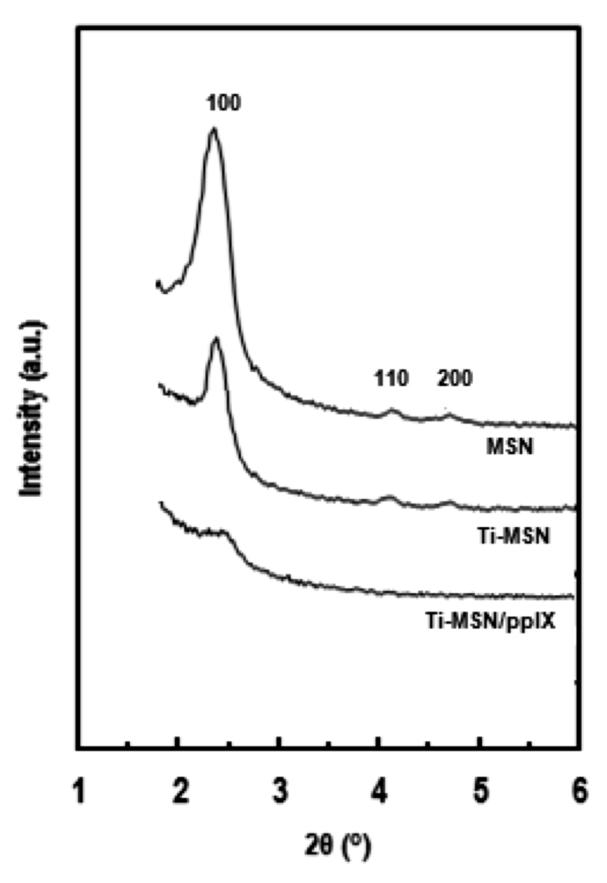


Fig. 2. XRD patterns of the MSN, Ti-MSN, and Ti-MSN/PpIX samples at Low degree region.

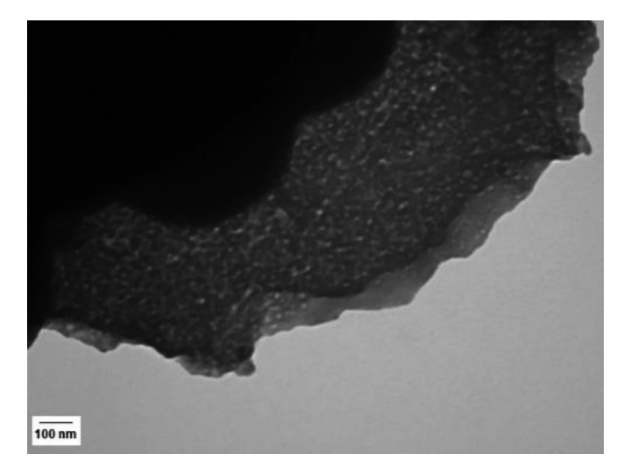


Fig. 3. TEM image of the Ti-MSN/PpIX catalyst.

with an average size of 50 nm–200 nm.

The spherical sizes changed by incorporating Ti and organic compound of PpIX. Two-dimensional hexagonal structure with d_{100} -spacing was about 3.5 nm with particle sizes of 70-110 nm.

DLS characterizations revealed that, Z-Average and Zeta potential of Ti-MSN/PpIX were 115.9 nm was -57.3 mV, respectively.

The hydrothermal stability of Ti-MSN was investigated at temperature of 600 °C in a reactor. The instrument was comprised of a temperature control, an airflow (100 mL/min) module and a water vapor generator. The Ti-MSN sample was heated initially under dry airflow to 473 K for 1 h then heating was continued to 600 °C under air saturated with water vapor for 2 h (heating rate of 2 K/min) and maintained at this temperature for 10 h. The results showed that no

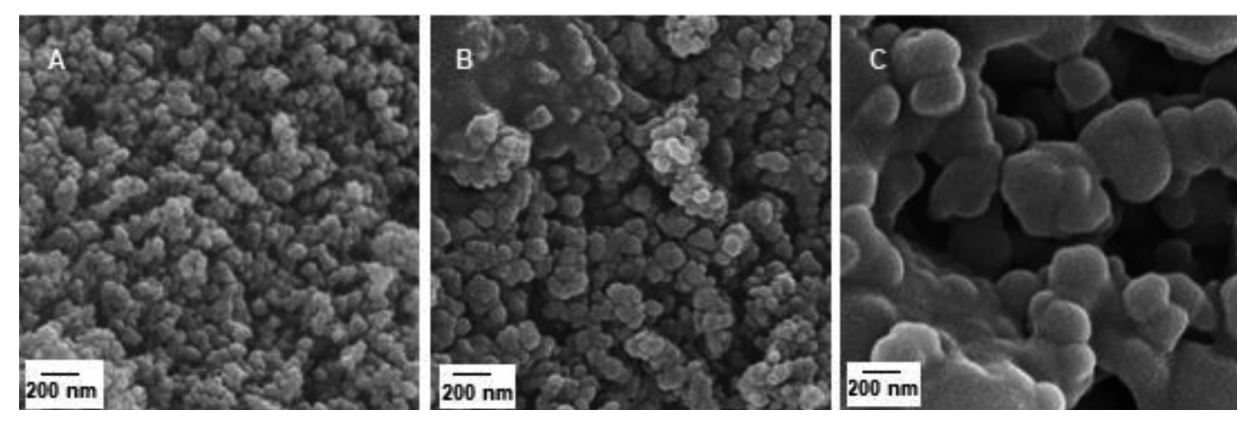


Fig. 4. SEM images of (A) MSN, (B) Ti-MSN, and (C) Ti-MSN/PpIX.

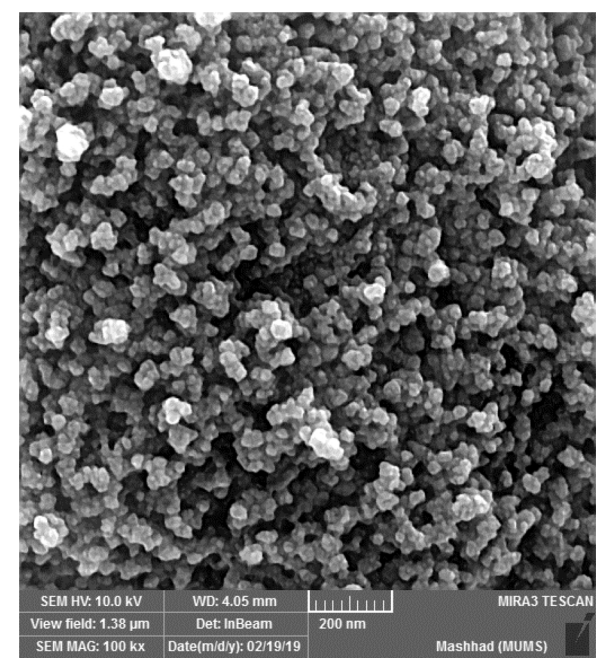


Fig. 5. FESEM image of Ti-MSN/PpIX.

specific difference in the main diffraction peak of the XRD patterns, before and after hydrothermal stability test, (Fig. 6) was observed.

The surface area of the MSN and composite are 995 and 204 m 2 g $^{-1}$, respectively. Introduction of titanium oxide and PpIX drastically reduced the surface area. In addition, grafting of Ti species and the organic molecule have plugged the MSN pores around 3–5 nm. The blocking pores decreased the total pore volume from 0.84 to 0.26 cm 3 g $^{-1}$. Decrease of d_{100} -spacing value and unit cell parameter confirmed the immobilizing of Ti and PpIX in the framework and the change in the composite structure [17].

The FT-IR spectra of pure MSN, Ti-MSN and Ti-MSN/PpIX composite are shown in Fig. 7. The stretching vibration of the silanol groups (Si-OH) was observed in the region of 3435 cm⁻¹ which is evident for the presence of the H-bonding in the structure [18]. Incorporation of titanium atoms and PpIX as an organic compound reduced the intensity of this bond for the Ti-MSN and composite. This was an indicative to the formation of new bonds between hydroxyl group and Ti atoms, and also PpIX molecules.

Two peaks at 2990 and 2851 cm⁻¹ are attributed to the C–H stretching due to the presence of PpIX in the composite structure. The vibration bonds of FTIR spectrum located at the regions of 465 and 1068 cm⁻¹ are corresponding to the vibrations of O–SiO and SiOS–––i, respectively. Whereas, the absorption peak at 796 cm⁻¹

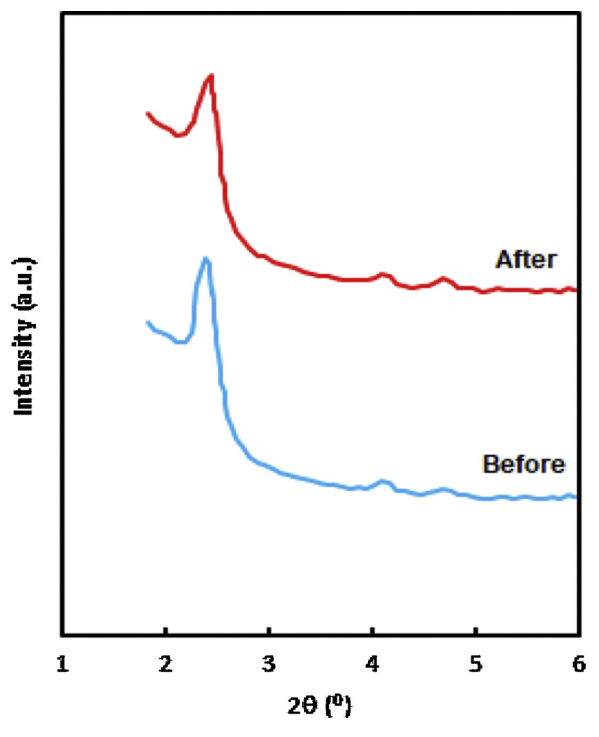


Fig. 6. XRD patterns of the Ti-MSN catalyst before and after hydrothermal stability test.

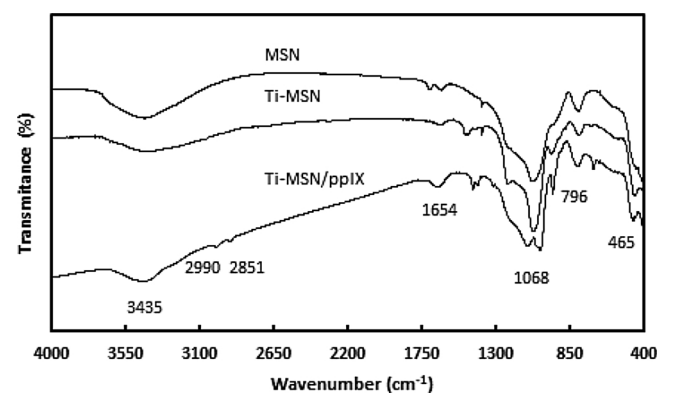


Fig. 7. FTIR spectra of MSN, Ti-MSN and Ti-MSN/PpIX.

indicated to the Si–OS–i bending vibration in the structures [19]. All the samples show the symmetric stretching vibration bond of Si–OSi at around 796 cm $^-$ -1 and the asymmetric vibration bond at around 1068

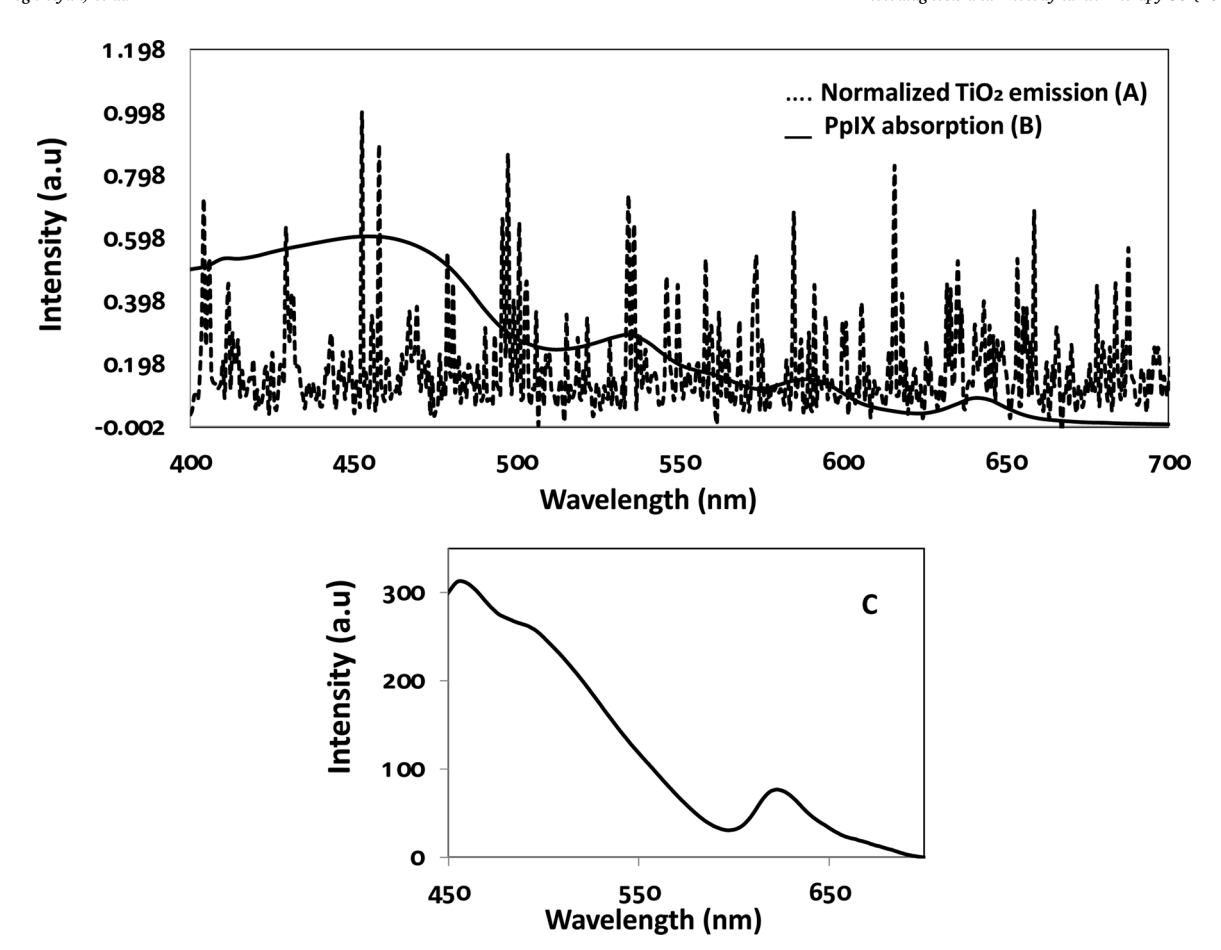


Fig. 8. A. The normalized emission spectra of TiO2 nanoparticles when activated by X-ray. B. The absorption spectrum of PpIX with the concentration of 12.5 μ M in DMSO.C. Detecting the fluorescence of PpIX by exciting the Ti-MSN/PpIX nanoparticles with 405 nm wavelength.

cm $^{-1}$. The bond at 469 cm $^{-1}$ allocated to the bending modes of Si–OS-i bond. Titanium species introduced to MSN and a slight red shift was observed at 1068 and 912 cm $^{-1}$ due to the strong interactions between titanium atoms and silicon (Ti–OS-i) [20].

3.2. Photodynamic activity of the composite

A prerequisite for energy transfer is to have an overlap between the light absorption spectrum of PpIX and emission spectrum of ${\rm TiO_2}$ nanoparticles (Anatase grade) when activated by X-ray (Fig. 8A & B). The luminescence of PpIX was detected by spectrofluorimetry of Ti-MSN/PpIX nanoparticles when activated by 405 nm wavelength (Fig. 8c).

PpIX absorption spectrum in the range of 400–700 nm was recorded by UV–vis spectrophotometer, its absorption spectrum has a strong absorption band around 445 nm (Soret band) and weaker Q bands peaking at 535, 590, and 645 nm. As Fig. 8 shows, the emission spectrum of $\rm TiO_2$ nanoparticles was largely overlapped with the absorption spectrum of PpIX.

Table 1 and Fig. 9 show the emission spectra of TiO₂ and Ti-MSN/PpIX nanoparticles while activated by X-ray.

Normalized emission spectrum (to a maximum) of Ti-MSN, and Ti-MSN/PpIX nanoparticles are presented in Fig. 8(a-d). The spectral intervals shown in Fig. 10(a-d) are related to the absorption of PpIX recorded in Fig. 8.

3.3. In vitro experiments

Cell viability assays were carried out using different concentrations of Ti-MSN/PpIX nanoparticles, and showed no cytotoxicity for concentrations up to 3.19 mg/mL (Fig. 11).

Spectral integral of TiO₂ and Ti-MSN/PpIX nanoparticles obtained from area under the curve in different spectral intervals of PpIX absorption spectrum.

Spectral range (nm)	Spectral integral		
	TiO ₂	Nanocomposite containing PpIX	
435 – 475 525 – 545 580 – 600 635 – 655	$55,447.4 \pm 13,414$ $30,199.1 \pm 14,139$ $25,800.7 \pm 5583$ $32,716.2 \pm 14,369$	$23,994.07 \pm 10,727$ $14,864.3 \pm 6442$ $17,765.8 \pm 7462$ $80,16.5 \pm 5150$	

3.4. X-PDT findings

As shown in Fig. 12, the toxicity of nanocomposite and Ti-MSN were not significant rather than control group.

The cell viability or survival fraction was calculated for each group relatively to the unirradiated control group. ANOVA and Tukey test as post hoc were used for statistical analysis. The survival fraction of the group incubated with Ti-MSN/PpIX nanoparticles, in the presence of X-ray, was significantly lower than in the absence of X-ray (p-value < 0.024). At 100 KVp energy of X ray, by increasing the radiation dose, decrease of cell survival was observed for the group incubated with Ti-MSN/PpIX nanoparticles, but they did not show significant difference with the group receiving only X-ray.

By irradiation at 100 cGy and 200 cGy doses, the reduction in cell viability of the group incubated with Ti-MSN/PpIX nanoparticles, was significantly higher than the group received only X-ray (P-value < 0.004) which confirmed the X-PDT. The survival fraction of the group received Ti-MSN/PpIX nanoparticles and 100 cGy dose was less than of

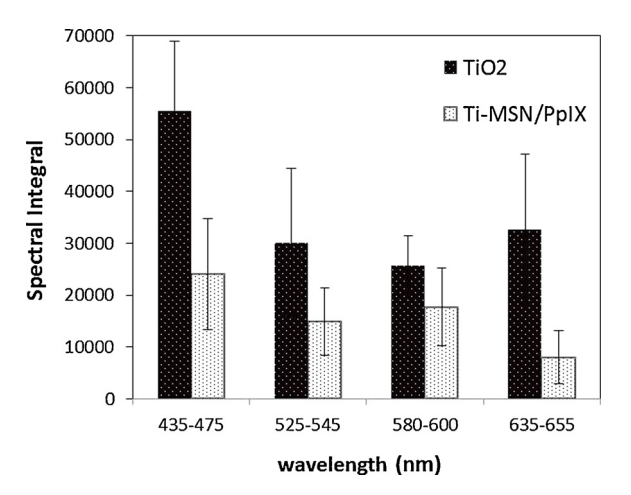


Fig. 9. The comparison of TiO_2 and Ti-MSN/PpIX nanoparticles on the basis of area under the curve (Spectral Integral) in different spectral intervals of PpIX absorption spectrum.

the group received only X-ray with 400 cGy dose; however, its difference was not significant (Fig. 13).

These results revealed that, increase the X-Ray did not change the cell viability once they were treated with X-PDT. Thus, 100 cGy might be considered as an optimized radiation dose for X-PDT at practical concentrations of these nanoparticles once irradiated with 6 MVp.

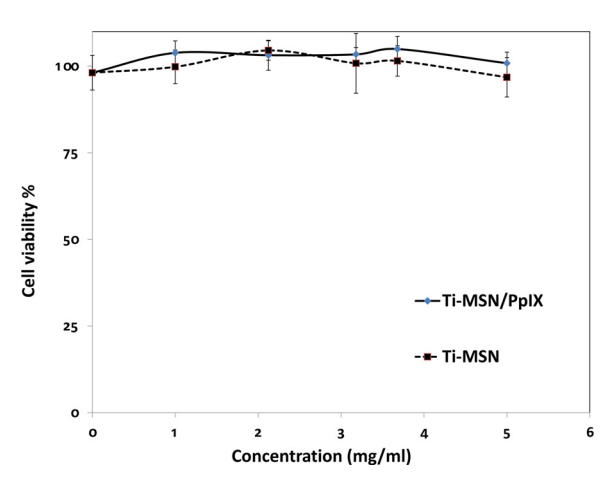


Fig. 11. Cell viability at different concentrations of Ti-MSN and Ti-MSN/PpIX nanoparticles. The cells were treated with varying concentrations of nanoparticles and incubated for 3 h. The data are expressed as mean \pm standard deviation for triplicate observations from three independent experiments.

The results obtained from comparison of 100 kVp and 6 MVp energies showed, the statistically significant difference between the group received Ti-MSN/PpIX nanoparticle in 100 cGy dose of these two energies (P-Value = 0.005). The survival fraction of the group received Ti-MSN/PpIX nanoparticle and 100 cGy dose in 6 MVp energy was less than the same group in 100KVp energy. The results indicated that, the

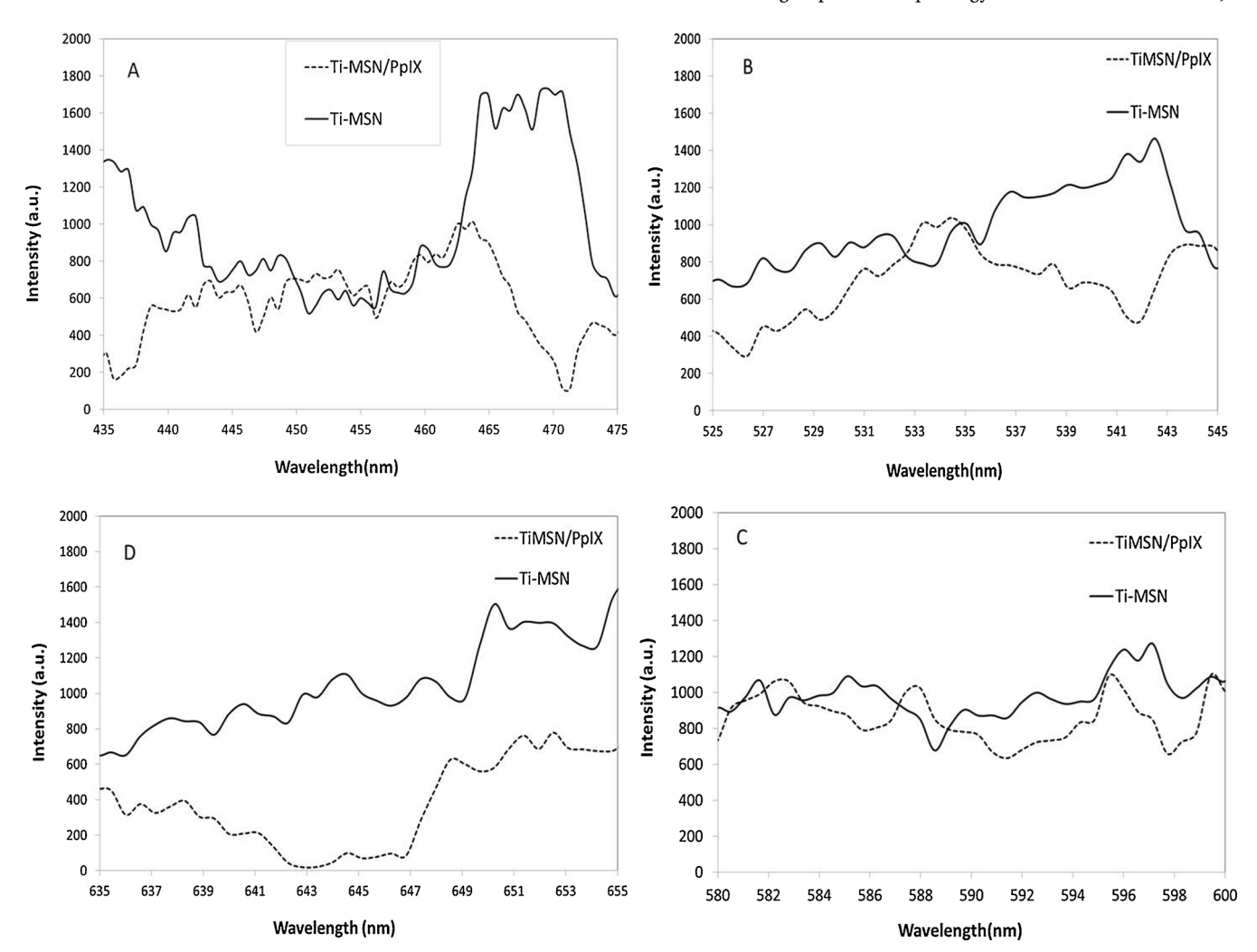


Fig. 10. (A-D). The emission spectrum of Ti-MSN and Ti-MSN/PpIX nanoparticles, when activated by X-ray in the intervals of PpIX absorption.

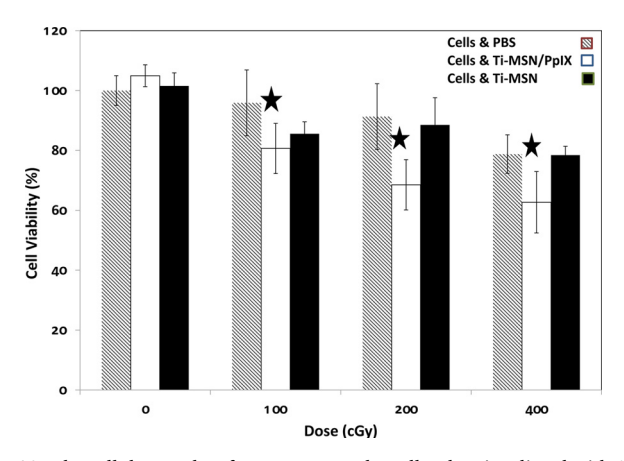


Fig. 12. The cellular results of MTT assay on the cells when irradiated with 100 kVp X-ray photons. The concentration of Ti-MSN/PpIX nanoparticle was 3.68 mg/mL and the incubation time was 3 h. The cells were analyzed by MTT assay after 48 h of exposure. The averages of three experiments formed the data. *Statistically significant difference compared with the group received Ti-MSN/PpIX nanoparticle alone (p < 0.05 using Tukey test).

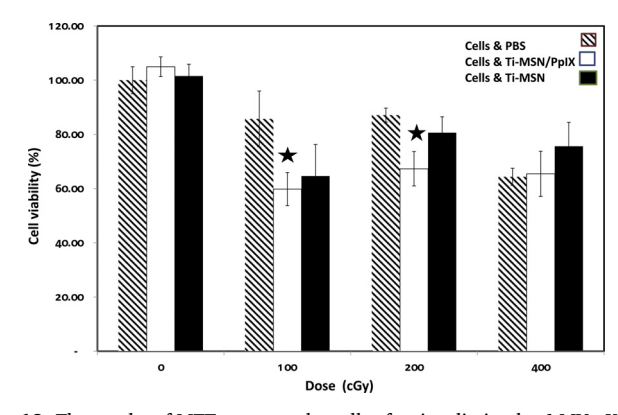


Fig. 13. The results of MTT assay on the cells after irradiation by 6 MVp X-ray photons. Cell viability was significantly reduced when cells were treated with X-PDT (Ti-MSN/PpIX nanoparticles plus X-ray) The concentration of Ti-MSN/PpIX nanoparticle was 3.68 mg/mL and the incubation time was 3 h.The cells were analyzed by MTT assay after 48 h of exposure. The averages of three experiments formed the data. *Statistically significant difference compared with the group received only x-ray (p < 0.05 using Tukey test).

use of Ti-MSN/PpIX nanoparticles in 6 MVp energy and 100 cGy dose, had an effective effect on treatment. While without the nanoparticles, the groups received only X-ray in these two energies did not differ significantly (P-Value = 1.000).

To compare the radiation effects, the radiation enhancement ratio (ER) for each energy and dose was calculated. ER was defined as the ratio of cell viability between X-ray group to X-PDT group. The ER was achieved 1.43 fold for 6 MVp energy and 100 cGy dose (Table 2).

4. Discussions

PDT and RT target different cellular components. For example, RT targets DNA while the target point of PDT is cell membrane. Such features cause the greater cytotoxicity as compared with only use of RT

Table 2
The enhancement ratio (ER) of both energies in each dose.

Dose (cGy)	ER of 6 MVp	ER of 100 KVp
100	1.43	1.20
200	1.28	1.33
400	0.98	1.23

or PDT. The combination of these modalities showed a promising treatment approach for cell lines which are resistant to RT, or deep seated tumors that cannot be treated with traditional PDT. Importantly, X-PDT can be viewed as a novel radio sensitizing technology.

The present study shows the synthesis and characterization of a new nanocomposite (Ti-MSN/PpIX nanoparticles) for X-ray induced photodynamic therapy aimed at combination of RT and PDT.

Nanotechnology can facilitate the communication between RT and PDT. The designed nanoparticles are PpIX and TiO2 carriers. TiO2 which is the agent of energy transfer from X-ray to UV/visible light, activates the loaded PpIX. The energy transfer from Ti-MSN nanoparticles to PpIX molecules was confirmed by the emission spectra of TiO₂ and Ti-MSN/PpIX nanoparticles, when activated by X-ray (illustrate in Table 1 and Fig. 9). Largely overlapped between the emission spectrum of TiO2 nanoparticles, when activated by X-ray, with all absorption wavelengths of PpIX especially with strong absorption band (Soret band) was one of the most important results of this study. This was the proof of the energy transfer and implementation of PDT before cellular tests. These results are comparable with Xiaoju Zou and et al. [26]. The emission spectrum of their nanoparticles overlapped with a peak at 520 nm of PpIX absorption spectrum. Our reported TiO2 nanoparticles had different emission peaks in PpIX absorption peaks, especially at 400 nm, which is very impressive in induced PDT. Therefore, the election of TiO2 along with PpIX was the correct selection, because the photo-emission of TiO2 was absorbed by PpIX and based on the prediction, PDT was occurred by utilizing X-ray irradiation. On the other, in previous studies it was shown that both PpIX and TiO₂ were radio sensitizers as well [21-23]. In this research, we employed two properties of radio and photo sensitizing of TiO2 and PpIX for the first time in X-PDT.

Ti-MSN/PpIX nanoparticles were not cytotoxic in the absence of X-ray irradiation that makes them suitable for medical applications. The structure of the Ti-MSN/PpIX nanoparticles was biocompatible due to use mesoporous silica nanoparticles. MSNs have high load capacity of drugs and they are biocompatible, too[24,25]. Also, the reason for using silica as a substrate was its transparency against light which does not absorb the light emitted from TiO₂.

These results revealed that the predicted hypothesis was realized through the use of X-ray. On the other words, by X-ray irradiation, ${\rm TiO_2}$ nanoparticles are activated and emit the spectrum of light which has the absorbance wavelength of PpIX. Theses light waves are absorbed by PpIX and photodynamic phenomenon is occurred. The reduction of cell survival fraction confirms the occurrence of photodynamic effects, as well. Higher rate of cell death can be associated with photodynamic therapy that originates from absorption of ${\rm TiO_2}$ emission wavelengths by PpIX.

After using the Ti-MSN/PpIX nanoparticles for the two energies, the results showed, the presence of the nanoparticles in 6 MVp energy had a great effect than 100 KVp energy. More interesting, the difference was in low dose of irradiation. This occurrence causes reduction of current dose in RT.

Generalov et al. [27] showed 1.5-fold increase in the radiation of $\rm ZnO/SiO_2$ nanoparticles for Du145 cells, which was in agreement with the reported results in the present study. This finding shows that the use of the proposed nano composite and X-ray induced photodynamic therapy results in radiation dose reduction. Thus it is a promising approach to use X-PDT for improved RT efficacy with reduced X-ray dose exposure to healthy tissue, for the treatment of radio resistant tumors.

5. Conclusion

Our findings show high cytotoxicity in the presence of Ti-MSN/PpIX nanocomposite and X-ray rather than radiation alone. Using Ti-MSN/PpIX nanoparticles decreases the required radiation dose. Hence, the proposed nanoparticle could be further improved as a relatively potent sensitizer for PDT to provide more treatment depth as well as a radio

sensitizer in the future.

Acknowledgements

This paper was extracted from a PhD thesis conducted at Medical Physics. The authors would like to thank the Research Deputy of MUMS for financial support under grant number of 951562. Also, the authors appreciate Samaneh Soudmand Salarabadi for cell culture education, Mr. Khatibzadeh and Mr. Hajhosseinian for their supports to conduct X-ray irradiation trials.

References

- [1] I.J. Macdonald, T.J. Dougherty, Basic principles of photodynamic therapy, J. Porphyr. Phthalocyan. 5 (2001) 105–129.
- [2] T. Hasan, B. Ortel, N. Solban, B. Pogue, Photodynamic therapy of cancer, Cancer Med. 7 (2003) 537–548.
- [3] W.J. Mulder, G.J. Strijkers, G.A. Van Tilborg, D.P. Cormode, Z.A. Fayad, K. Nicolay, Nanoparticulate assemblies of amphiphiles and diagnostically active materials for multimodality imaging, Acc. Chem. Res. 42 (2009) 904–914.
- [4] Y. Wang, Q. Zhao, Y. Hu, L. Sun, L. Bai, T. Jiang, S. Wang, Ordered nanoporous silica as carriers for improved delivery of water insoluble drugs: a comparative study between three dimensional and two dimensional macroporous silica, Int. J. Nanomed. 8 (2013) 4015.
- [5] G.D. Wang, H.T. Nguyen, H. Chen, P.B. Cox, L. Wang, K. Nagata, Z. Hao, A. Wang, Z. Li, J. Xie, X-ray induced photodynamic therapy: a combination of radiotherapy and photodynamic therapy, Theranostics 6 (2016) 2295.
- [6] W. Chen, J. Zhang, Using nanoparticles to enable simultaneous radiation and photodynamic therapies for cancer treatment, J. Nanosci. Nanotechnol. 6 (2006) 1159–1166
- [7] J. Xu, J. Gao, Q. Wei, Combination of photodynamic therapy with radiotherapy for cancer treatment. J. Nanomater. 2016 (2016).
- [8] J.H. Pinthus, A. Bogaards, R. Weersink, B.C. Wilson, J. Trachtenberg, Photodynamic therapy for urological malignancies: past to current approaches, J. Urol. 175 (2006) 1201–1207.
- [9] P. Couleaud, V. Morosini, C. Frochot, S. Richeter, L. Raehm, J.-O. Durand, Silica-based nanoparticles for photodynamic therapy applications, Nanoscale 2 (2010) 1083–1095.
- [10] S.-H. Cheng, C.-H. Lee, M.-C. Chen, J.S. Souris, F.-G. Tseng, C.-S. Yang, C.-Y. Mou, C.-T. Chen, L.-W. Lo, Tri-functionalization of mesoporous silica nanoparticles for comprehensive cancer theranostics—the trio of imaging, targeting and therapy, J. Mater. Chem. 20 (2010) 6149–6157.
- [11] H.S. Qian, H.C. Guo, P.C.L. Ho, R. Mahendran, Y. Zhang, Mesoporous-silica-coated up-conversion fluorescent nanoparticles for photodynamic therapy, Small 5 (2009)

- 2285-2290.
- [12] J. Zhu, H. Wang, L. Liao, L. Zhao, L. Zhou, M. Yu, Y. Wang, B. Liu, C. Yu, Small mesoporous silica nanoparticles as carriers for enhanced photodynamic therapy, Chem. – Asian J. 6 (2011) 2332–2338.
- [13] G. Blasse, Scintillator materials, Chem. Mater. 6 (1994) 1465-1475.
- [14] W. Yang, P.W. Read, J. Mi, J.M. Baisden, K.A. Reardon, J.M. Larner, B.P. Helmke, K. Sheng, Semiconductor nanoparticles as energy mediators for photosensitizerenhanced radiotherapy, Int. J. Radiat. Oncol. Biol. Phys. 72 (2008) 633–635.
- [15] N. Kamarudin, A. Jalil, S. Triwahyono, V. Artika, N. Salleh, A. Karim, N. Jaafar, M. Sazegar, R. Mukti, B. Hameed, Variation of the crystal growth of mesoporous silica nanoparticles and the evaluation to ibuprofen loading and release, J. Colloid Interface Sci. 421 (2014) 6–13.
- [16] M. Aziz, A. Jalil, S. Triwahyono, R. Mukti, Y. Taufiq-Yap, M. Sazegar, Highly active Ni-promoted mesostructured silica nanoparticles for CO2 methanation, Appl. Catal. B: Environ. 147 (2014) 359–368.
- [17] M.R. Sazegar, A. Dadvand, A. Mahmoudi, Novel protonated Fe-containing mesoporous silica nanoparticle catalyst: excellent performance cyclohexane oxidation, RSC Adv. 7 (2017) 27506–27514.
- [18] E.H. Kim, Y. Ahn, H.S. Lee, Biomedical applications of superparamagnetic iron oxide nanoparticles encapsulated within chitosan, J. Alloys Compd. 434 (2007) 633–636.
- [19] K. Alipour, F. Nasirpouri, Smart anti-corrosion self-healing zinc metal-based molybdate functionalized-mesoporous-silica (MCM-41) nanocomposite coatings, RSC Adv. 7 (2017) 51879–51887.
- [20] B. Li, N. Wu, K. Wu, J. Liu, C. Han, X. Li, Bimetallic V and Ti incorporated MCM-41 molecular sieves and their catalytic properties, RSC Adv. 5 (2015) 16598–16603.
- [21] J. Yamamoto, S. Ogura, T. Tanaka, T. Kitagawa, Y. Nakano, T. Saito, M. Takahashi, D. Akiba, S. Nishizawa, Radiosensitizing effect of 5-aminolevulinic acid-induced protoporphyrin IX in glioma cells in vitro, Oncol. Rep. 27 (2012) 1748.
- [22] M. Rezaei-Tavirani, E. Dolat, H. Hasanzadeh, S. Seyyedi, V. Semnani, et al., TiO₂ nanoparticle as a sensitizer drug in radiotherapy: in vitro study, Int. J. Cancer Manag. 6 (Supplement) (2013) e80460.
- [23] M. Bakhshizadeh, S.A. Mohajeri, H. Esmaily, S.A. Aledavood, F.V. Tabrizi, M. Seifi, F. Hadizadeh, A. Sazgarnia, Utilizing photosensitizing and radiosensitizing properties of TiO2-based mitoxantrone imprinted nanopolymer in fibrosarcoma and melanoma cells. Photodiagnosis Photodvn. Ther. 25 (2019) 472–479.
- [24] J. Xi, J. Qin, L. Fan, Chondroitin sulfate functionalized mesostructured silica nanoparticles as biocompatible carriers for drug delivery, Int. J. Nanomed. 7 (2012) 5235
- [25] H. Huang, C. Ong, J. Guo, T. White, M.S. Tse, O.K. Tan, Pt surface modification of SnO 2 nanorod arrays for CO and H 2 sensors. Nanoscale 2 (2010) 1203–1207.
- [26] X. Zou, M. Yao, L. Ma, M. Hossu, X. Han, P. Juzenas, W. Chen, X-ray-induced nanoparticle-based photodynamic therapy of cancer, Nanomedicine 9 (2014) 2339–2351.
- [27] R. Generalov, W.B. Kuan, W. Chen, S. Kristensen, P. Juzenas, Radiosensitizing effect of zinc oxide and silica nanocomposites on cancer cells, Colloids Surf. B: Biointerfaces 129 (2015) 79–86.